

FEASIBILITY STUDY OF ADJOINT INVERSE MODELING OF ASIAN DUST USING LIDAR NETWORK OBSERVATIONS

Itsushi Uno⁽¹⁾, Keiya Yumimoto⁽¹⁾, Nobuo Sugimoto⁽²⁾,
Atsushi Shimizu⁽²⁾ and Shinsuke Satake⁽³⁾

⁽¹⁾ Research Institute for Applied Mechanics, Kyushu Univ., Fukuoka, Japan

⁽²⁾ National Institute for Environ. Studies, Tsukuba, Japan

⁽³⁾ Research Institute for Humanity and Nature, Kyoto, Japan

ABSTRACT

Feasibility of a four-dimensional variational (4DVAR) data assimilation system for regional dust modeling is described. We applied this model for optimization of dust emissions in East Asia using NIES LIDAR network observations during the dust episode of 30 April 2005. Optimized dust emissions improved under-prediction of dust concentrations and brought assimilated concentrations into better agreement with LIDAR observations, but that agreement is not perfect. We obtained an 18% increase of dust emission by data assimilation, especially over the Mongolian region. The assimilated results indicate that the 4DVAR method is very powerful for unification of observation and modeling. It yields better forecasting capability.

1. INTRODUCTION

Dust emission and transport modeling is important for elucidating the recent increase of Asian dust episodes. Recent dust models [1-3] have reproduced many important observational facts and have given valuable information to elucidate characteristics of Asian dust phenomena. Results of the recent dust model inter-comparison project (DMIP [4]) provide several important directions for the future study of Asian dust modeling and observations. One important conclusion is that the dust emissions from Mongolia and Inner Mongolia have been only sparsely measured, are highly model-dependent, and require more observations and consensus within the dust modeling community. Therefore, methods for unification of observation and modeling play a salient role in improving the dust forecasting capability in Asia.

Four-dimensional variational (4DVAR) data assimilation method, based on the adjoint model, provides solutions to various underlying problems of numerical models (e.g., initial conditions and emissions). Such data assimilation methods have been used in meteorological and oceanographic modeling. Recently, 4DVAR method has come to be applied to chemical transport models (CTMs) for inverse modeling. Various observations are used in conjunction with CTMs to evaluate emissions of several chemical species and to optimize model parameters. For example, Müller and Sravralou [5] estimated CO and NO_x emissions using the adjoint version of a global IMAGE model from ground-based and GOME satellite observations. Hakami

et al. [6] estimated black-carbon emissions over eastern Asia using the adjoint STEM-CTM model. However, applications of 4DVAR method for CTMs remain limited; the method remains in a developmental stage.

We developed RAMS/CFORS [7] based on a 3D on-line regional scale CTM that was fully coupled with Regional Atmospheric Modeling System (RAMS [8]). Based on that successful CTM, we are developing a new 4DVAR data assimilation system. The 4DVAR version of CTM is a very powerful tool to elucidate the proper dust emission and transport. A real-time combination of CTM-4DVAR and LIDAR measurement would play an important role in the next generation of Asian dust observation-modeling networks. In this paper, we will present first-stage results of adjoint inverse modeling of Asian dust using NIES LIDAR network observations to assess the feasibility of 4DVAR modeling in dust modeling. Here, we will simplify dust modeling, using one dust particle bin, and restrict our first application to the extreme dust episode of 30 April 2005 in Sendai Japan, as reported by [9].

2. RAMS/CFORS AND ADJOINT MODEL

The chemical transport model of RAMS/CFORS [7] is designed as a multi-tracer, on-line system built within the RAMS. The mass conservation equation is

$$\rho_{air} \left\{ \frac{\partial}{\partial t} Q_a + \text{div}(Q_a \cdot \mathbf{v}) \right\} = F_{diff} + F_{grav} + F_{react} + F_{emis} + F_{dry} + F_{wet} \quad (1)$$

where ρ_{air} represents the air density, Q_a is the gas/aerosol mixing ratio, and \mathbf{v} is the 3-D wind velocity vector. Also, F_{diff} , F_{grav} , F_{react} , F_{emis} , F_{dry} and F_{wet} respectively signify the turbulent diffusion, gravitational settling, chemical reaction/conversion, emission, and dry/wet deposition tendency of gas/aerosols.

Mineral aerosols in CFORS are injected into the atmosphere by high-velocity surface winds. In this study, one bin dust particle (assuming 2- μm diameter) are modeled, and the total dust uplift flux is calculated on-line using a fourth power-law function of surface friction velocity u_* as

$$F_{dust} = C u_*^3 (u_* - u_{*,th}), \quad (2)$$

where C is the emission constant (function of surface condition; and which can be optimized using 4DVAR) and $u_{*,th}$ is the threshold friction velocity. Natural dust emission areas are defined as desert and semi-desert

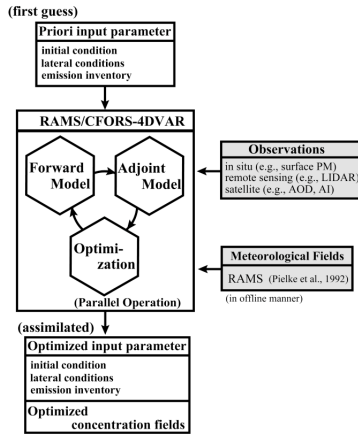


Fig. 1 Schematic of the RAMS/CFORS-4DVAR data assimilation system

areas from the 1-km resolution land-cover characteristics produced by the U.S. Geological Survey (USGS).

Based on this forward mode RAMS/CFORS, we developed the adjoint inverse model. A schematic diagram of RAMS/CFORS-4DVAR is shown in Fig. 1.

In 4DVAR data assimilations, a cost (objective) function must be defined. This takes the form of a quadratic scalar function, which is generally defined as follows.

$$J(\mathbf{C}) = \frac{1}{2}(\mathbf{C} - \mathbf{C}_b)^T \mathbf{B}^{-1}(\mathbf{C} - \mathbf{C}_b) + \frac{1}{2} \sum_{i=1}^n (H_i \mathbf{C} - \mathbf{y}(t_i))^T \mathbf{R}^{-1}(H_i \mathbf{C} - \mathbf{y}(t_i)) \quad (3)$$

The first term on the right hand side represents a departure of the assimilated value \mathbf{C} from the first guess (before data assimilation) value \mathbf{C}_b , weighted by the background error covariance (\mathbf{B}). The second term represents the discrepancies between simulated and observed concentrations weighted by the observation error covariance (\mathbf{R}). The observation operator H represents the forward model and the transformation from \mathbf{C} into observation \mathbf{y} .

Minimization of the cost function J , $\partial J / \partial \mathbf{C} \rightarrow \min$, is performed through iterative integrations of the forward and adjoint models, which entails a huge numerical load and much computing time. To reduce this computational cost, RAMS generates meteorological fields in advance; these generated meteorological fields drive the forward and adjoint models in an off-line manner.

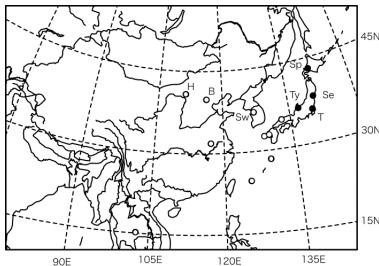


Fig. 2 Modeling domain and observation sites of NIES LIDAR network; Tsukuba (T), Sapporo (Sp), Sendai (Se), Toyama (Ty), Suwon (Sw), Beijing (B), and Hohhot (H).

The numerical model domain is centered at 25°N, 115°E on a rotated polar stereographic system. The horizontal grid comprises 100 × 90 grid points with a resolution of 80 km; Fig. 2 shows the subdomain of x grids from 1 to 90 and y grids from 30 to 90. The model's vertical domain extends from the surface to 23 km with 22 stretching grid layers. The RAMS is a regional meteorological model that requires initial and boundary meteorological conditions. In this study, NCEP/NCAR reanalysis data, with 2.5° × 2.5° resolution were used for lateral and initial boundary conditions of RAMS. Here, RAMS/CFORS-4DVAR was applied for the period of 26 April – 1 May 2005 with zero initial dust concentration. More details of RAMS/CTM-4DVAR are reported in [10].

3. OBSERVATION DATA

LIDARs are useful tools for measuring vertical profiles of aerosols with high spatial and temporal resolution. They provide important dust time-height data continuously [11]. Especially, the NIES LIDAR network uses LIDARs that measure backscattering at 532 nm and 1064 nm, and the depolarization ratio at 532 nm. Currently, the NIES LIDARs are operated continuously at the following 12 locations (see Fig. 2). The vertical observation resolution is 30 m. The LIDAR signals are converted to aerosol extinction intensity. Details of this method are described in [11-12].

The RAMS/CFORS-4DVAR can use the dust extinction coefficient directly to evaluate the cost function, but in this feasibility study, we decided to use the dust concentration (mixing ratio). Therefore, the mass concentration of dust is estimated from the mass/extinction conversion factor. The conversion factor for typical dust case in Beijing was estimated as 1.78 g m⁻² [12]; this value is used. However, this conversion factor is dependent on particle size and is probably much smaller for the transported dust with smaller sizes.

Within NIES LIDAR network points, we used only four sites (Sendai, Sapporo, Toyama, and Tsukuba; shown in bold circles in Fig. 2) for 4DVAR calculation. Note that only one time slice observation datum at Sapporo was used in 4DVAR because of numerous missing observations. A validation of the assimilation results by observations that were not used in the assimilation is crucially important. Sites such as Hohhot, Beijing, and Suwon are used for independent model evaluation. The cost function of 4DVAR is evaluated with a 3 h interval. Therefore, LIDAR data are vertically interpolated to RAMS vertical axis. Then 1-h averaged LIDAR data are used in 4DVAR calculations.

4. RESULTS AND DISCUSSION

As written in the Introduction, we specifically examined the RAMS/CFORS-4DVAR application to the heavy dust episode that occurred on 30 April 2005 in the northern part of Japan, especially at Sendai City.

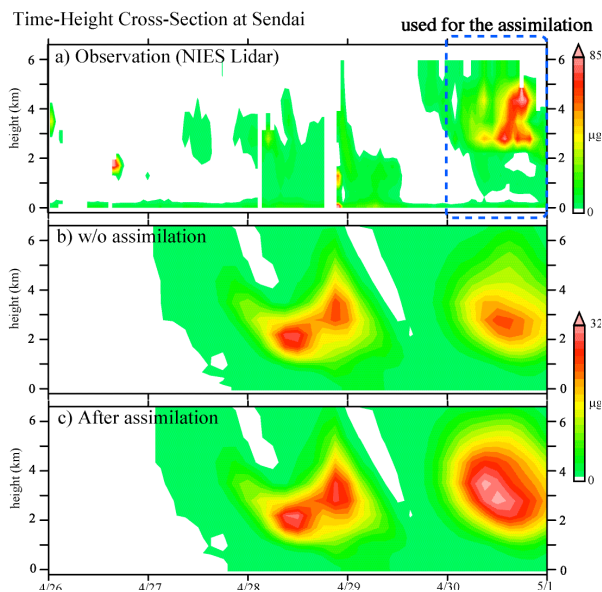


Fig. 3 Time-height cross-section of dust concentration at Sendai (a) LIDAR observation, (b) modeled without data assimilation, (c) modeled with data assimilation.

Fig. 3 shows a time-height cross-section of observed and simulated dust concentrations at Sendai. **Fig. 3(a)** shows the dust concentration observed by NIES LIDAR. A very dense dust layer aloft is clearly visible. This thick dust layer that appeared on 30 April was $z=3-5$ km. The maximum extinction coefficient reaches 1 km^{-1} , which corresponds to several hundred micrograms per cubic meter. A similar dust layer was observed in Sapporo, Tsukuba, and Toyama during the same period [12]. **Fig. 3(b)** shows simple forward simulation results (without assimilation) based on the ACE-Asia version of RAMS/CFORS model. **Fig. 3(c)** is the result after assimilation.

In general, the dust concentrations without assimilation capture the overall behavior and variation of the observations (despite a missing observation). However, differences between the simulated and observed concentrations are considerable. The assimilated result improved the presence of the elevated dust layer (both height and concentration) on 30 April. This brings modeled concentration values closer to observed ones. However, the values are still smaller than the observations; they cannot reproduce the thin dust layer structure perfectly.

Fig. 4 shows an examination of vertical profiles between the observed and simulated dust concentration at Sendai, Toyama, Tsukuba, Sapporo, Beijing, and Hohhot. The comparison data correspond to the period when the high dust-layer concentration was observed in each site (24 h on 30 April for Japanese sites, and on 28 April for Chinese sites). Observations take the bottom axis and model results are shown on the upper axis for

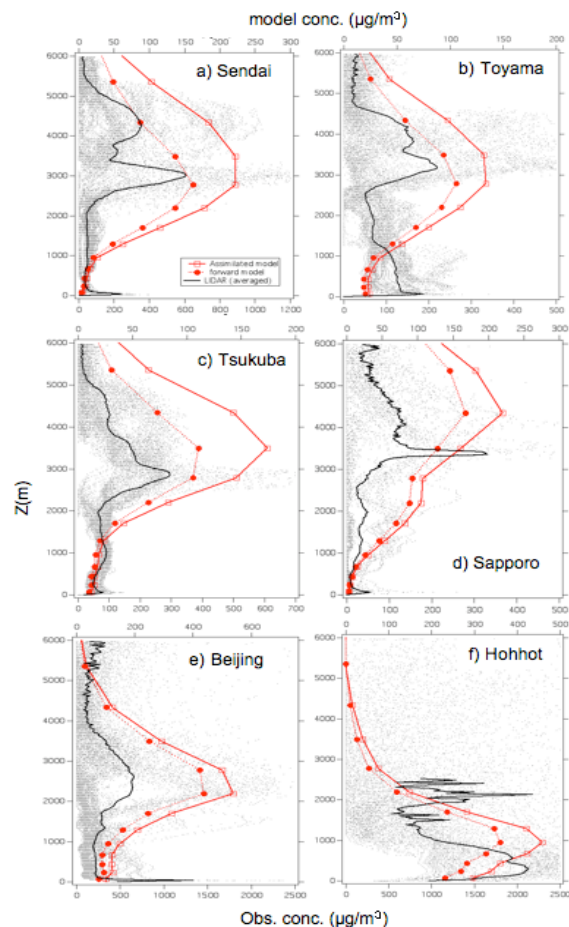


Fig. 4 Vertical profile of dust concentration. Dot is 5 min averaged LIDAR data. The blue thick line is the 24 h averaged LIDAR profile. The red dashed line is the 24 h averaged model profile without data assimilation. The red solid line is the 24 h averaged model profile with data assimilation. (a) Sendai, (b) Toyama, (c) Tsukuba, (d) Sapporo, (e) Beijing, and (f) Hohhot.

shown as dots; the 24-h average is shown as a black solid line. The assimilation result clearly compensates under-predictions of the simulation results and improves their mean concentration and peak level height (except for Sapporo). In general, assimilation results increase the concentration level approximately 30–40%, but it remains difficult to retrieve a sharp concentration peak because of the rough vertical model resolution.

For Sendai, assimilation results increased the concentration level, but it is still not sufficient to reproduce the observed sharp profile. Several reasons for this problem exist. One reason is that the horizontal resolution of 80 km and thickness of the vertical layer might not be sufficient to reproduce this thin elevated dust layer. Another reason is the assumption of a one-bin dust model together with the single mass/extinction conversion factor (Sendai is located in the far-downwind

region from the dust source region, so the proper conversion ratio might differ slightly).

For Sapporo, assimilated results failed and worked for the opposite direction (it becomes higher than observation). This is true because the available observation in Sapporo is quite limited and 4DVAR might not work strongly to correct the concentration in Sapporo. It might also be related to the vertical grid spacing (the observation shows a distinct dust peak aloft), and the setting of the error covariance matrix of **B** and **R**. This point requires further study.

For independent evaluation sites, assimilation results work well for Beijing and Suwon (not shown in the figure). The result of Hohhot does not change greatly because this site is near the source region and its observed concentration level is very high (1–2 mg/m³). Moreover, the coarse dust fraction might be dominant, whereas our one bin dust model assumes a diameter of 2 μm. Therefore, more complete examination near dust source regions requires the use of the multi-bin model, which is the next step of our model development.

The assimilated results reflect markedly increased dust emissions from Mongolia, especially from the western side of Mongolia (not shown in Fig). For that reason, under-predictions might result from insufficient dust emissions from Mongolia. Our data assimilation indicates that the total optimized dust emission during this dust episode must be approximately 18% higher than the original CFORS estimates.

5. CONCLUDING REMARKS

We applied a 4DVAR data assimilation system for optimization of dust emissions in the East Asian region using NIES LIDAR network observations during the dust episode that occurred on 30 April 2005. The first feasibility study of RAMS/CTM-4DVAR was demonstrated. We found the following:

1. Optimized dust emissions improved under-prediction of dust concentrations and brought assimilated concentrations into better agreement with LIDAR observations; nevertheless, the agreement is not yet perfect.
2. Results showing dust assimilation indicated increased dust emissions in Mongolia. We obtained an 18% increase of dust emissions using data assimilation, especially over the Mongolia region.
3. In this study, we only used four LIDAR observation sites in Japan, which are all very distant from the dust source regions. The assimilated results agree with the TOMS AI distribution (not shown in Fig) and indicate that the 4DVAR method is very powerful for unification of observation and modeling; it therefore provides better forecasting capability.

In this study, we restricted our observation data to those from the LIDAR network. However, 4DVAR method is very capable of including surface level observations (such as PM₁₀, SPM) and satellite retrievals (e.g., aerosol optical depth (AOD), Aerosol Index). The inclusion of

these data (as well as introduction of a multi-particle dust bin) will improve the dust model capability markedly and will be the next step of 4DVAR application.

Acknowledgements

This work was partly supported by the Global Environmental Research Fund, Ministry of Environment, Japan and the Grant-in-Aid for Scientific Research under Grant No.17360259 from Ministry of Education, Culture, Sports, Science and Technology, Japan.

References

1. Gong, S. L., et al., Characterization of soil dust aerosol in China and its transport and distribution during 2001 ACE-Asia: Part 2 Model simulation and validation, *J. Geophys. Res.*, 108, 4262, doi:10.1029/2002JD002633, 2003.
2. Shao, Y., et al., Numerical prediction of northeast Asian dust storms using an integrated wind erosion modeling system, *J. Geophys. Res.*, 107, doi:10.1029/2001JD001493, 2002.
3. Uno et al., Numerical Study of Asian Dust Transport during the Springtime of 2001 simulated with the CFORS model, *J. Geophys. Res.*, 109, doi:10.1029/2003JD004222, 2004.
4. Uno et al., Dust model intercomparison (DMIP) study over Asia - Overview, *J. Geophys. Res.*, 2005JD006575, 2006 (in press).
5. Müller, J.-F., Stavrou, T., Inversion of CO and NO_x emissions using the adjoint of the IMAGES model. *Atmospheric Chemistry and Physics* 2, 67-78, 2005.
6. Hakami et al., Adjoint inverse modeling of black carbon during the Asian Pacific Regional Aerosol Characterization Experiment. *J. Geophys. Res.*, 110 D14301, 2005.
7. Uno et al., Regional Chemical Weather Forecasting System CFORS: Model Descriptions and Analysis of Surface Observations at Japanese Island Stations During the ACE-Asia Experiment, *J. Geophys. Res.*, 108, doi:10.1029/2002JD002845, 2003.
8. Pielke, R. A. et al., A comprehensive meteorological modeling system: RAMS. *Meteorology and Atmospheric Physics* 49, 69–91, 1992.
9. Sugimoto et al., Asian dust phenomenon of April 30, 2005 in Sendai observed by Lidar, Tenki, 2005 (in Japanese)
10. Yumimoto, K. and I. Uno, Adjoint inverse modeling of CO emissions over the East Asian region using four dimensional variational data assimilation, accepted in *Atmos. Environ.*, 2006.
11. Shimizu et al., Continuous observations of Asian dust and other aerosols by dual-polarization lidars in China and Japan during ACE-Asia. *J. Geophys. Res.*, 109, doi:10.1029/2002JD003253, 2004.
12. Sugimoto et al., Record heavy Asian dust in Beijing in 2002: Observations and model analysis of recent events, *Geophys. Res. Lett.*, 30, doi:10.1029/2002GL016349, 2003.